Photocatalytic Hydrogen Production from Homo- and Hetero-geneous Cobalt (II) Catalysts

Ayni Sharif

Under the supervision of Professor Darrin Richeson

A undergraduate thesis submitted to the University of Ottawa in partial fulfillment of the requirements for the degree of Honours Bachelor of Science in Biomedical Sciences

Department of Chemistry and Bimolecular Sciences

Faculty of Science

University of Ottawa

Ayni Sharif

Abstract

Various energy sources on which society depends are rapidly depleting in recent years. Alternate fuel sources that are cost efficient, earth abundant, and easily accessible has been urgently sought out by numerous researchers worldwide. Hydrogen represents an excellent target that could meet these pressing needs. This project has identified efficient photocatalytic production of hydrogen from the reduction of water using both homo- and hetero-geneous cobalt (II) complexes. A pincer selenium-nitrogen ligand scaffold, 2,6-bis[(pyrazol-1-yl)methyl]pyridine, was used to support a potential homogeneous catalyst. However, the formation of precipitates during catalytic process raised concerns over certainty of the activity of the homogeneous catalyst. These concerns prompted the investigation of cobalt oxide nanoparticles as potential heterogeneous catalysts. These explorations revealed this system to be a much more efficient catalyst through visible-light photochemistry of reducing water for hydrogen production in the presence of a $Ru(bpy)_3^{2+}$ photosensitizer and a reductant.

Table of Contents

1. Introduction

The rapid depletion of heavily dependant non-renewable energy sources poses a threat to the environment[1]. Due to its toxic gases, an eco-friendly, cost efficient, and renewable alternative is urgently needed[2]. An energy resource that is practical, earth abundant, and easily accessible points to hydrogen as an ideal alternative fuel source. In recent years, photocatalytic water splitting has gained attraction in the field of hydrogen generation since hydrogen can be extracted in means of artificial photosynthesis where renewable resources of sunlight and water are used[3]. Using solar energy to produce a usable form of energy is a very noteworthy feat since light is relatively equally distributed on the planet, very abundant, strictly nonpolluting, virtually inexhaustible, and free[4].

Water splitting produces molecular hydrogen as a potential alternative fuel source by using sunlight to excite suspended semiconductor particles[5-7]. Various theories have been hypothesized and tested with what water is actually reduced to, yet only a small subgroup were able to give evidence of the occurrence of a catalytic reaction. One of the more prevalent theories of hydrogen production with water is that hydrogen is reduced to give hydrogen gas and oxygen is oxidized to give oxygen gas with a molar ratio of 2:1 respectively[8]. This reaction would provide society with an unlimited source of hydrogen, which is a clean, energy rich solar fuel. Pure water splitting in regards with powdered heterogeneous catalysts is expected to produce hydrogen and oxygen gas[8].

In the case of photocatalytic water splitting, a catalyst absorbs photon energy and consequently, electrons are transferred from its valence band to its conduction band. If its band gap is large enough, above that needed for water splitting (1.23 eV), and its band edges meet the thermodynamic requirement for the charge transfer to occur, then in principle, excited electrons can reduce hydrogen ions and holes can oxidize oxygen anions[8]. For the photocatalytic water splitting reaction to occur, an electron donor and photosensitizer are necessary to drive and enhance the yield of hydrogen generation[9].

In natural photosynthesis, water is commonly seen as the sacrificial electron donor, fuelling the natural photosystem with electrons by oxidizing oxygen to generate biological reductants such as NADPH and by reducing carbon dioxide[10]. A similar sacrificial electron donor is needed in artificial photosynthesis. However, water as an electron donor in photocatalysis raises numerous difficulties, thus alternatives are used[11]. Essentially, an electron donor is needed to fuel a reductive photosystem with needed electrons and, in particular with this study, to generate hydrogen.

Correspondingly, a photosensitizer absorbs a photon, excites an electron in the species to a higher energy level, and simultaneously leaves an unoccupied site at a lower energy[12]. As a result the photosensitizer is now both a stronger reductant and a stronger oxidant than when it was in the ground state[12]. The electron coming from the excited electron in the photosensitizer can reduce a component in the system[12]. Alternatively, the empty electronic state, which is a hole, in the photosensitizer can function as an oxidant[12]. Fundamentally, the photosensitizer is need in the

photosystem since it is the component that absorbs the light when being irradiated in photocatalysis and therefore, making the photocatalytic reduction of water possible.

The most central component of photocatalytic water splitting is arguably the catalyst. There are a broad family of both homogenous and heterogeneous catalysts. Homogeneous molecular photocatalysts have been exploited in the preparation of hydrogen gas evolution for a variety of cobalt complexes[9]. Pyridine based cobalt homogeneous catalysts showed to be the most efficient in the generation of hydrogen[9]. Still, even with various categories of photocatalytic materials being explored in literature for hydrogen production, metal oxides are of high interest[12].

After the invention of photo-electrochemical water splitting in 1972 by Fujishima and Honda, nearly 9000 research articles have been published, outlining the use of various photocatalysts[13]. In particular, nanoparticles have been studied in recent years and has particularly been studied for many applications of energy and environmental significance[14-16]. The unique physical and chemical properties of nanoparticles make it a noteworthy alternative in various environmental applications. The properties of nano-materials have a profound effect in heterogeneous photocatalysis[17]. Photocatalytic hydrogen generation with nanoparticles has been reported in the literature and since cobalt based catalysts have been extensively researched in hydrogen generation as well, cobalt nanoparticles is the ideal avenue to explore[17-18]. Granted that cobalt is less abundant

than other transition metals, it is still emerging as a potential metal for catalytic processes owing to its light harvesting and electron mediating properties.

The Co_3O_4 nanoparticle as a heterogeneous catalyst has been previously reported for its water splitting ability in producing hydrogen gas[19-20]. In a review paper, Artero et al. have discussed the role of cobalt-based compounds towards hydrogen generation rate, stating that it holds remarkable potential in hydrogen production[21]. The cobalt heterogeneous catalysts remain relatively unexplored regardless of their reported potential in hydrogen production.

Our interest lay in exploring homo- and hetero-geneous cobalt catalyst variations with the goal of forming novel hydrogen generation catalysts. Cobalt based catalysts were synthesized and evaluated through photocatalytic activity in hydrogen generation. The amount of hydrogen generation of the homogeneous and heterogeneous catalysts was compared, which revealed that the cobalt nanoparticle produced significantly more hydrogen. The effect of various photocatalytic conditions in hydrogen production was also studied meticulously for both catalyst types.

2. Experimental

2.1. *General Methods*

Reactions were performed in a glove box under a nitrogen atmosphere, with the exception of the ligand synthesis, which was performed using standard Schlenk techniques under a flow of nitrogen and also the nanoparticles, which was done in normal atmosphere conditions. All solvents were either purchased dry from Sigma-Aldrich or were purged with nitrogen and then dried by passage through a column of activated alumina using an apparatus purchased from Anhydrous Engineering. All other chemicals were purchased from Sigma-Aldrich and used without further purification.

2.2. *A Standard Photochemistry Experiment*

In a nitrogen filled glove box, a 20 mL glass vial with a magnetic stirrer bar was filled with either catalyst **1** or **2** and $[Ru(bpy)_3]^{2+}$ photosensitizer. These were dissolved in 4 mL of dry dimethylformamide (DMF). This solution was combined with either 1-Benzyl-1,4-dihydronicotinamide (BNAH, 1 mmol), triethanol amine (TEOA, 1 mL), and/or triethylamine (TEA, 1 mL) as the sacrificial electron donor. The vial was sealed and removed from the glove box. To this solution, 0.2 mL of water that was purged with nitrogen was added with a syringe. The solution was further purged with nitrogen for five minutes and then irradiated using 450 nm blue LED lights (radiant flux at 700 mA of 1050 mW) for 24 hours. The amount of hydrogen produced in the headspace of the vial was obtained using gas chromatograph analysis.

2.3. *Synthesis*

2.3.1. *Synthesis of 2,6-Bis[(pyrazol-1-yl)methyl]pyridine Ligand*

The procedure was modeled after a previously published protocol[22]. A solution of diphenyl diselenide (0.32 g, 1 mmol) in 30 mL of ethanol was stirred under a nitrogen atmosphere. Sodium borohydride (0.076 g, 2 mmol) dissolved in 5 mL of aqueous sodium hydroxide (5%) was added to the diphenyl diselenide solution drop wise until it became colourless due to the formation of PhSeNa. 2,6-Bis-(chloromethyl)pyridine (0.176 g, 1 mmol) dissolved in 10 mL of ethanol was added to the colorless solution with constant stirring and the mixture was stirred further for 3 hours. It was then poured into cold water (30 mL). The ligand was extracted with chloroform (4x25 mL) from the aqueous layer. The extract was washed with water (3x40 mL) and dried over anhydrous sodium sulphate. The solvent was evaporated off under reduced pressure on a rotary evaporator to result in a viscous oil, which on mixing with methanol (5 to 7 mL) and placing in a refrigerator (5°C) gave single crystals of the Se-N-Se Ligand.

2.3.2. *Synthesis of Cobalt (II) 2,6-Bis[(pyrazol-1-yl)methyl]pyridine Complex [**1**]*

Cobalt (II) bromide (0.219 g, 1 mmol) was mixed in a 1:1 molar ratio with the Se-N-Se ligand (0.417g, 1 mmol) in a 20 mL vial. Under a nitrogen atmosphere, the two solids were dissolved in 10 mL of DMF to form a dark blue homogenous liquid complex (0.2 mol/L). The solution was stirred further for 16 hours giving the cobalt (II) Se-N-Se complex **1**.

2.3.3. *Synthesis of Cobalt Oxide (CoO_x) Nanoparticles [**2**]*

The procedure was modeled after a previously published protocol[23]. Cobalt (II) nitrate hexahydrate (0.582 g, 2 mmol) was mixed in a 2:5 molar ratio with ammonium bicarbonate (0.395 g, 5 mmol) in an agate mortar and pestle. At room temperature, the two solids were mixed and milled to quickly produce a purple foamy paste releasing ammonia and carbon dioxide. The colour of the composition changed regularly while it was milled for 30 minutes, finally producing a grey solid with no more colour changes. The solid was then washed with distilled water (5 x 20 mL), transferred to a ceramic crucible and left to dry in air at 100°C to produce the nanoparticle precursor. After drying, the precursor was calcined under air at 300°C for 2 hours to obtain the cobalt oxide nanoparticles **2** as a fine black powder.

2.3.4. *Synthesis of Tris(2,2-bipyridine)ruthenium(II) hexafluorophosphate*

Ruthenium (III) chloride (0.539 g, 2.6 mmol) and 2,2-bypridine (2.49 g, 16mmol) were dissolved in 100 mL of ethanol with a stir bar. The mixture was heated to a reflux for 12 hours under a nitrogen atmosphere at 78°C. The mixture was cooled to room temperature and potassium hexafluorophosphate (1.8466 g, 10 mmol) was added. A red precipitate formed and this solid was collected by filtration, washed with distilled water (3 x 10 mL), and further washed with acetone (3 x 10 mL) to remove ruthenium salts. After removing all solvents, the red precipitate was placed in a vial and dried for 16 hours under vacuum to produce the $[Ru(bpy)_3]^{2+}$ photosensitizer.

3. Results and Discussion

3.1. *Characterization*

The original avenue of exploration to discover new catalysts for hydrogen production was based on pincer complexes of cobalt (II)[9]. Pincer ligand scaffolds are relatively new in being used as a supporting scaffold for catalytic hydrogen production. Rao et al. explored the possibilities of ligand variation to provide discovery of hydrogen evolving catalysts[9]. Using new cobalt (II) complexes supported by the neutral pincer ligand PN_3P, bis(diphenylphosphino)-2,6-di(methylamino)pyridine (Scheme 1), proved to photocatalytically reduce water to hydrogen in the presence of a $Ru(bpy)_3^{2+}$ photosensitizer and a reductant[9].

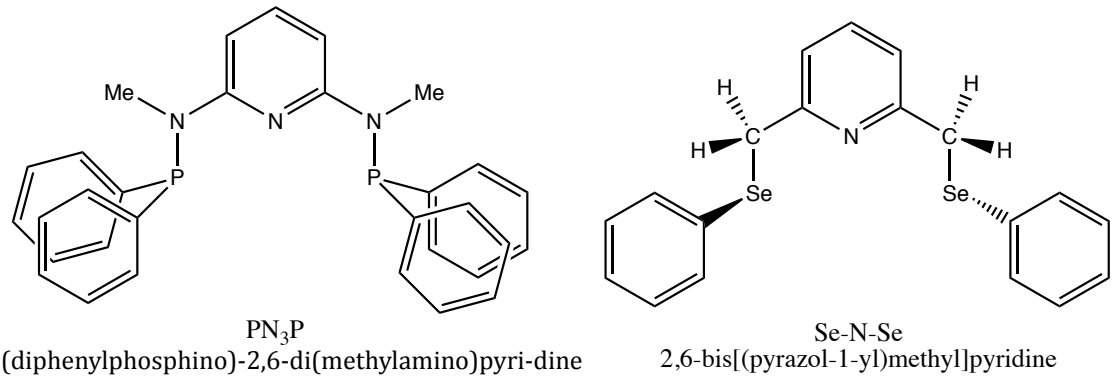

PN_3P
bis(diphenylphosphino)-2,6-di(methylamino)pyri-dine

Se-N-Se
2,6-bis[(pyrazol-1-yl)methyl]pyridine

Scheme 1. PN_3P and Se-N-Se ligand comparison.

Our interests lay in wanting to further expand and explore similar pincer scaffolds in hopes of designing new hydrogen generation catalysts that are able to reduce water into hydrogen. Pyridines in complexes, as with PN_3P, have been seen to be among efficient homogeneous catalysts for hydrogen generation from water[9]. Therefore, using the Se-N-Se scaffold ligand, which maintains the pyridyl core, has the flanking phosphorus phenyls units replaced with selenium phenyl units.

A ligand synthesis is summarized in Scheme 2. A reaction between 2,6-pyridinedimethanol and thionyl chloride was done to produce the intermediate for the Se-N-Se ligand. The intermediate was then reacted with diphenyl diselenium and a strong base, in this case sodium borohydride, to yield 2,6-bis[(pyrazol-1-yl)methyl]pyridine, Se-N-Se ligand, at 75% yield. The reaction was done in a nitrogen atmosphere in order to minimize the potential of oxygen acting as an oxidizer in the reaction.

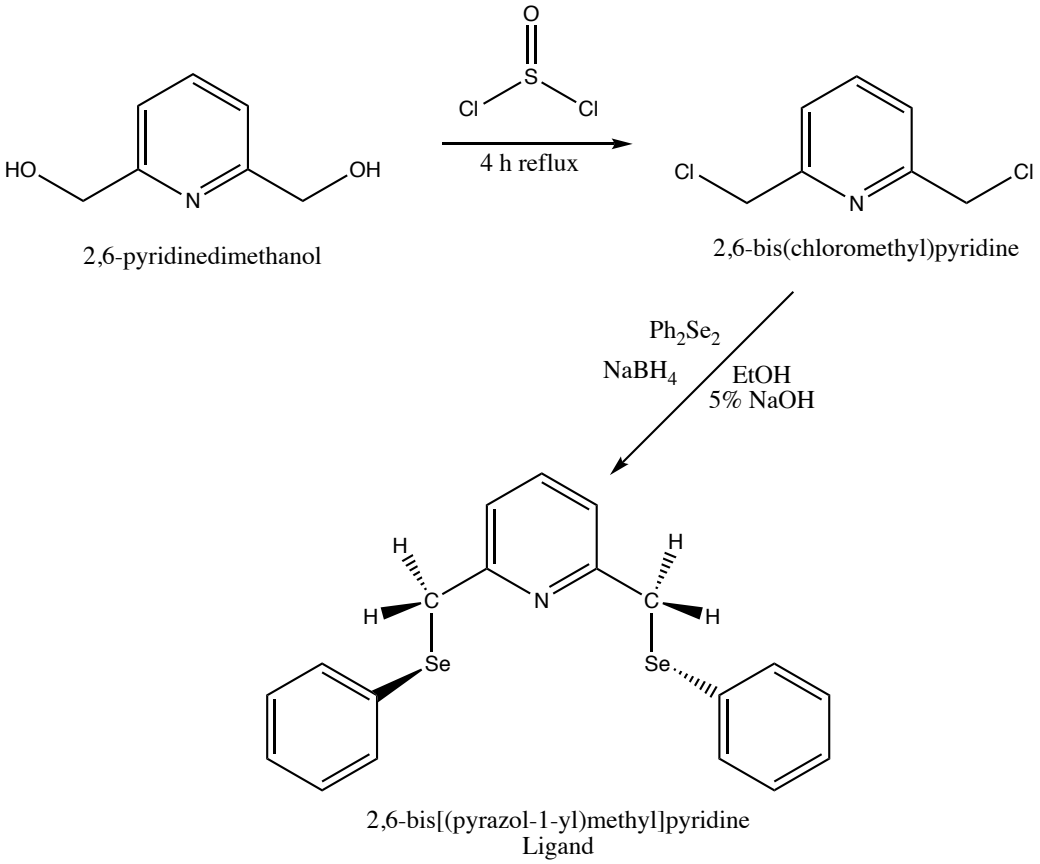

Scheme 2. Synthesis of Se-N-Se ligand.

Cobalt has been vastly exploited as the metal center for photocatalytic complexes in the field of hydrogen production[9, 17-18]. Therefore, 2,6-bis[(pyrazol-1-

yl)methyl]pyridine ligand was directly reacted with cobalt (II) bromide in a 1:1 molar ratio to obtain cobalt (II) as the metal center for the Se-N-Se ligand. This reaction was a very efficient reaction, which can be seen in Scheme 3 to produce [κ^3-Co(II)-$SeNSeBr_2$] (**1**) in 90% yield.

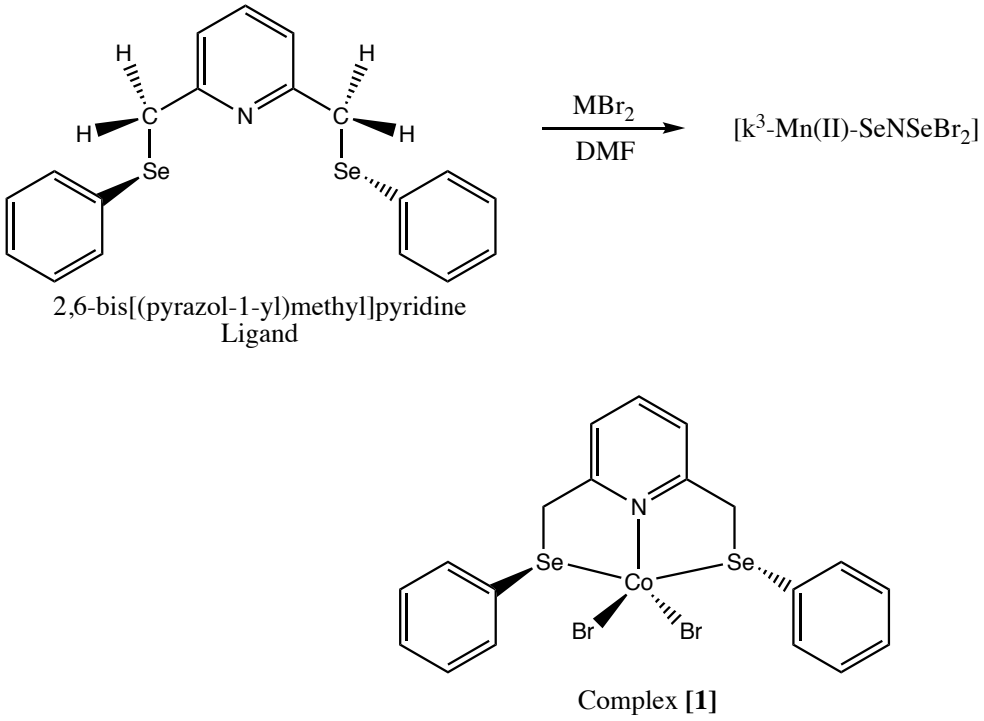

Scheme 3. Synthesis of [κ3-Co(II)-SeNSeBr2] complex **1**.

As seen in Scheme 4, a crystal structure was obtained of complex **1** by using the common vapour crystallization method, where the inner vial solvent was toluene and the outer vial solvent was hexane. The crystals were obtained by X-ray diffraction analysis, which revealed a molecular shape of a rough square pyramidal at the cobalt center, which has an identical bonding structure as the product seen in Scheme 3.

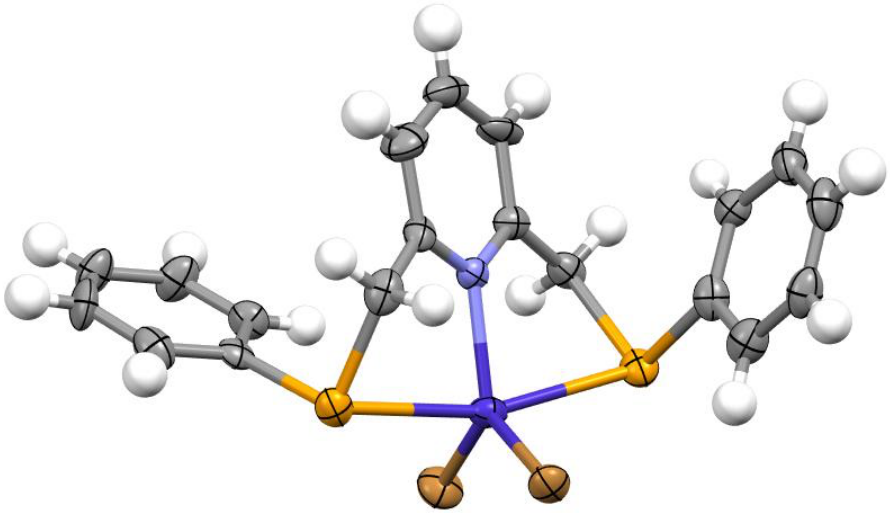

Scheme 4. [κ3-Co(II)-SeNSeBr$_2$] **1** crystal structure.

3.2. *Photocatalytic Potential of Cobalt (II) Complex*

The synthesized cobalt Se-N-Se complex was evaluated for its photocatalytic activity for hydrogen production through a water splitting reaction. The experiment was done under a nitrogen atmosphere and irradiated under the visible light spectrum of 450 nm blue LED lights. The amount of hydrogen generated was analysed with gas chromatography with the carrier gas being argon. The data for hydrogen generation for the synthesized cobalt Se-N-Se complex is presented below in Tables 3-6, 8-9, 11, and 14.

Each sample contained cobalt Se-N-Se catalyst, $Ru(bpy)_3^{2+}$ photosensitizer, a sacrificial reductant, organic solvent, and water as the proton source. When initially mixed, the sample was a homogeneous soluble light red solution. After being irradiated with 450 nm blue lights for a period of time, the sample changed to a dark green solution and a black granule precipitate formed. Seeing the black precipitate

form for various conditions using catalyst **1** raised concern on the impact of the system and therefore demanded attention.

Speculating that the precipitate arose from the cobalt catalyst **1** that was used, the black precipitate was filtered out from an irradiated sample and used in place of the catalyst **1** under similar photocatalytic conditions. The results can be seen in Table 1.

Table 1. Summary of the results for the photocatalytic production of hydrogen using [k^3-Co(II)-$SeNSeBr_2$] or the filtered precipitate as the catalyst in dimethylformamide (DMF) with $[Ru(bpy)_3]^{2+}$ as the photosensitizer. Distilled water (H_2O) was used as the proton source. The electron donor used was 1 mL of triethanolamine (TEOA). Irradiation with 450 nm lights was conducted on solution under a nitrogen atmosphere for 24 hours. The lights were positioned at each of the four corners coming from the sides to the vials.

[1] (μmol)	$Ru(bpy)_3^{2+}$ (μmol)	Solvent	Electron Donor	Additive	Irradiation Time	H_2 (μmol)
1	1	DMF	TEOA	H_2O (0.2 mL)	24 hr	93.222
Filtered precipitate	1	DMF	TEOA	H_2O (0.2 mL)	24 hr	23.533

This heterogeneous system could also generate hydrogen, producing approximately 25% of the amount compared to the original sample that generated the new precipitated catalyst. An additional observation of these reactions was that the pH of the reaction solution tested to be slightly basic. This observation led us to speculate that the precipitate was likely coming from formation of cobalt (II) hydroxide with the hydroxide arising as a by-product from the reduction of H^+ from water. Hydroxide then has the high potential of reacting with cobalt (II) to form cobalt (II) hydroxide, which is illustrated in Scheme 5. With this being the case, the precipitate can be seen to hinder the maximum potential of hydrogen that can be produced.

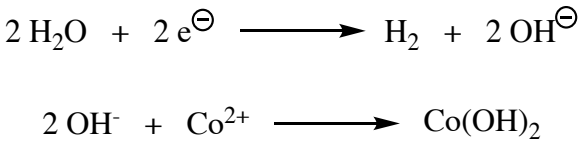

Scheme 5. Cobalt (II) hydroxide formation from reduction of water.

These observations and hypotheses motivated the exploration of a new avenue of heterogeneous cobalt catalysts instead of a homogeneous catalyst. This required a catalyst precursor that was more precisely defined and analyzed than the precipitate that was obtained. Since the time frame remaining for these series of experiments was limited, it was thought best to use the time efficiently and wisely by using a known heterogeneous cobalt material[12]. It was decided to make cobalt oxide (CoO_x) nanoparticles (**2**) as the heterogeneous catalyst.

The nanoparticles were synthesized by directly reacting cobalt (II) nitrate hexahydrate in a 2:5 molar ratio with ammonium bicarbonate. This reaction, which can be seen in Scheme 6, produces a fine black powder of cobalt oxide nanoparticles (**2**) as the product in 80% yield.

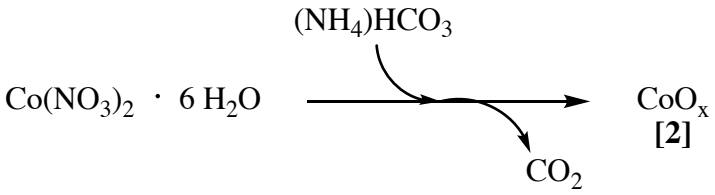

Scheme 6. Synthesis of CoO_x nanoparticles.

The nanoparticles were subjected to analysis through an X-ray diffraction as can be seen in Scheme 7. This diffraction spectrum yielded broad reflections with spacings consistent with formation of small crystallites of Co_3O_4. The size of the particles was

analyzed using the Scherrer equation, which is a formula that relates the size of submicrometre crystallites in a solid to the broadening of a peak in a diffraction pattern. This equation is used in determining the size of the crystals in the form of powder. The Scherrer equation can be written as:

$$\beta = \frac{K\lambda}{L\cos\theta}$$

where L is the crystalline size, K is the Scherrer constant, λ is the X-ray wavelength, β is the line broadening at half the maximum intensity (FWHM), and θ is the angle of diffraction (Bragg angle).

The constant of proportionality, K, depends on how the width is determined, the shape of the crystal, and the size distribution. The most common value for K is 0.94 for FWHM of spherical crystals with cubic symmetry, but varies with the actual shape of the crystallite and could be rounded up to 1[24].

The peak width, due to crystallite size, varies inversely with crystallite size that is, as the crystallite size gets smaller, the broader the peak gets. In terms of crystallite size broadening, the peak width, β, varies with 2θ as cos θ, where the crystallite size broadening is most pronounced at large angles of 2θ and peak intensity is weakest at larger angles of 2θ[24].

In relations of using a single peak, using diffraction peaks between 30° and 50° for 2θ often produces better results, where below 30° for 2θ compromises profile analysis of the peak asymmetry[24].

Therefore, looking at Scheme 7, the black bars represent the angles and intensities of the known Co_3O_4 nanoparticles and the X-ray wavelength represents the powder diffraction of catalyst **2**. Seeing that the peaks of the X-ray closely lines up with the angles and intensities of Co_3O_4 nanoparticles confirms that the product that was formed in Scheme 6 was cobalt oxide nanoparticles, specifically Co_3O_4 nanoparticles.

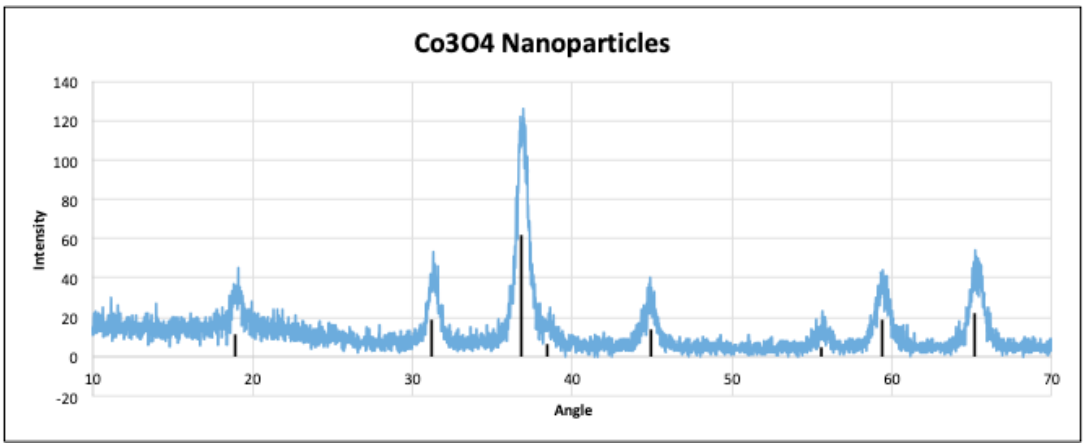

Scheme 7. X-ray powder diffraction data of the Cobalt Oxide (Co_3O_4) nanoparticles catalyst.

The numerical values of the peaks are seen in Table 2. The peaks of 2θ in Scheme 7 are in the first column of Table 2. The lines broadening at half the maximum intensity, FWHM, are seen in column four. Using the Scherrer equation, particle size, which is L from the equation, was calculated. This is seen in the last column of Table 2, where wavelength is 1.5406, K is 0.94, and radians for both theta and FWHM were used in the calculation. Averaging all eight calculated particle size results, gives an average particle size of approximately 100 Å or 10 nm for catalyst **2**.

Table 2. Summary of the X-ray powder diffraction data for Cobalt Oxide (Co_3O_4) nanoparticles.

2θ Peak in Degrees	θ in Degrees	θ in Radians	β (FWHM) in Degrees	β (FWHM) in Radians	Particle Size A in Angstroms
18.91	9.460	0.1650	0.75	0.01309	112.155
31.19	15.595	0.2722	0.76	0.01326	113.349
36.81	18.405	0.3212	0.87	0.01518	100.513
38.42	19.210	0.3353	0.89	0.01553	98.726
44.91	22.455	0.3919	0.94	0.01641	95.512
55.57	27.785	0.4849	1.12	0.01955	83.738
59.38	29.690	0.5182	0.98	0.01710	97.462
65.16	32.580	0.5686	1.01	0.01763	97.494
					99.869

3.3. *Effects of Various Parameters on Photocatalytic Generation*

3.3.1. *Effect of Illumination Intensity*

Photocatalytic reactions are influenced by the intensity and amount of absorption of light that occurs, as well as the duration of irradiation. The effect of illumination intensity on photocatalytic activity was studied by the amount of hydrogen generation based on the position of the 450 nm blue LED lights.

The first set of photocatalytic experiments took place with a single 450 nm blue LED light positioned underneath the sample facing upward. The sample was irradiated for 24 hours. These reactions can be seen in Table 3, where one sample had no catalyst **1** and the second sample has the catalyst **1**. There is an approximate 30% increase of hydrogen generation between the two reactions.

Table 3. Summary of the results for the photocatalytic production of hydrogen using [k³-Co(II)-SeNSeBr$_2$] in dimethylformamide (DMF) with [Ru(bpy)$_3$]$^{2+}$ as the photosensitizer. Distilled water (H_2O) was used as the proton source. The electron donor used was 1 mmol of 1-benzyl-1,4-dihydronicotinamide (BNAH). Irradiation with 450 nm lights was conducted on solution under a nitrogen atmosphere for 24 hours. The light was positioned directly under each vial.

[1] (µmol)	$Ru(bpy)_3^{2+}$ (µmol)	Solvent	Electron Donor	Additive	Irradiation Time	H_2 (µmol)
-	1	DMF	BNAH	H_2O (0.2 mL)	24 hr	12.176
1	1	DMF	BNAH	H_2O (0.2 mL)	24 hr	17.190

The second set of photocatalytic experiments took place with four 450 nm blue LED lights positioned at the four corners facing the sample. The sample was irradiated for 24 hours. These reactions can be seen in Table 4, where one sample had no catalyst **1** and the second sample has the catalyst **1**. There is a significant increase of about 92% between the two reactions.

Table 4. Summary of the results for the photocatalytic production of hydrogen using [k³-Co(II)-SeNSeBr$_2$] in dimethylformamide (DMF) with [Ru(bpy)$_3$]$^{2+}$ as the photosensitizer. Distilled water (H_2O) was used as the proton source. The electron donor used was 1 mmol of 1-benzyl-1,4-dihydronicotinamide (BNAH). Irradiation with 450 nm lights was conducted on solution under a nitrogen atmosphere for 24 hours. The lights were positioned at each of the four corners coming from the sides to the vials.

[1] (µmol)	$Ru(bpy)_3^{2+}$ (µmol)	Solvent	Electron Donor	Additive	Irradiation Time	H_2 (µmol)
-	1	DMF	BNAH	H_2O (0.2 mL)	24 hr	2.491
1	1	DMF	BNAH	H_2O (0.2 mL)	24 hr	29.765

When the samples containing catalyst **1** from Table 3 and 4 are compared, the latter position of lights generated 42% more hydrogen than when only one light was irradiating one sample. In addition, the background samples revealed less production in Table 4 than in Table 3. This encouraged subsequent reactions to be done in similar conditions that were set in place with results in Table 4.

The discrepancy between the results of Table 3 and 4 can be explained with the Lambert-Beer Law, which relates concerning the absorption of radiant energy by an absorbing medium[25]. The relationship can be expressed as $A = \varepsilon lc$ where A is absorbance, ε is the molar extinction coefficient, l is the length of the path light must travel in the solution, and c is the concentration of a given solution. The variables that come into play with the two different positioning explained in Table 3 and 4 are ε and A. Molar extinction coefficient, ε, is a measure of how strongly a chemical species or substance absorbs light at a particular wavelength[25]. The sample that is being irradiated with four 450 nm blue LED lights is absorbing the light at a greater strength than when a single 450 nm blue LED light is used because of the increase in the surface area the lights are covering. This in turn causes a direct increase in A, the absorbance outcome.

3.3.2. *Effect of Irradiation Time*

As mentioned previously, photocatalytic reactions are influenced by not only absorption of light but also the duration for which the sample is being irradiated for on the photocatalytic surface. The effect of irradiation time on photocatalytic activity was studied by performing a time profile of irradiation time. This was done with two different sacrificial donors, BNAH and TEOA, as well as with the two types of catalysts, **1** and **2**.

Using BNAH as the electron donor showed a direct relationship with irradiation time and hydrogen generation, the longer the sample was irradiated for the more production of hydrogen there was, which can be seen in Table 5. When irradiation

time was plotted against hydrogen production in Scheme 8, a logarithmic relationship is observed. This produced a reasonable R^2 value of 0.8176. There is a steady increase in hydrogen production as time goes on; the data suggests that a plateau will eventually be reached. This correlation is coherent since an unlimited amount of hydrogen production is near impossible especially in a closed environment of the sample with limited reactants.

Table 5. A time profile for the photocatalytic production of hydrogen using [k^3-Co(II)-$SeNSeBr_2$] in dimethylformamide (DMF) with $[Ru(bpy)_3]^{2+}$ as the photosensitizer. Distilled water (H_2O) was used as the proton source. The electron donor used was 1 mmol of 1-benzyl-1,4-dihydronicotinamide (BNAH). Irradiation with 450 nm lights was conducted on solution under a nitrogen atmosphere. The lights were positioned at each of the four corners coming from the sides to the vials.

[1] (µmol)	$Ru(bpy)_3^{2+}$ (µmol)	Solvent	Electron Donor	Additive	Irradiation Time	H_2 (µmol)
1	1	DMF	BNAH	H_2O (0.2 mL)	2 hr	13.733
1	1	DMF	BNAH	H_2O (0.2 mL)	4 hr	15.789
1	1	DMF	BNAH	H_2O (0.2 mL)	6 hr	48.584
1	1	DMF	BNAH	H_2O (0.2 mL)	8 hr	53.181
1	1	DMF	BNAH	H_2O (0.2 mL)	25 hr	60.453
1	1	DMF	BNAH	H_2O (0.2 mL)	48 hr	62.801
1	1	DMF	BNAH	H_2O (0.2 mL)	72 hr	69.977

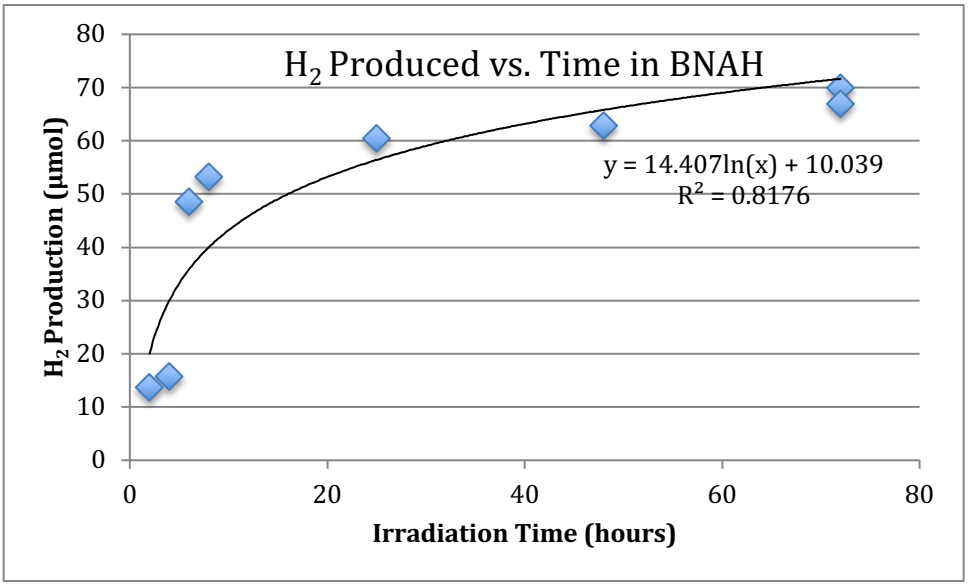

Scheme 8. A time profile for the photocatalytic production of hydrogen using [k³-Co(II)-SeNSeBr$_2$] in dimethylformamide (DMF) with [Ru(bpy)$_3$]$^{2+}$ as the photosensitizer. Distilled water (H_2O) was used as the proton source. The electron donor used was 1 mmol of 1-benzyl-1,4-dihydronicotinamide (BNAH). Irradiation with 450 nm lights was conducted on solution under a nitrogen atmosphere. The lights were positioned at each of the four corners coming from the sides to the vials.

Using TEOA as the electron donor also showed a direct relationship with irradiation time and hydrogen generation, the longer the sample was irradiated for the more production of hydrogen there was, which can be seen in Table 6. However, when irradiation time was plotted against hydrogen production in Scheme 9, a linear relationship is observed. This produces a remarkable R^2 value of 0.9886, nearly a value of 1. Looking at the data at face value suggests no plateau will be reached. Instead it suggests the that there will be an unlimited amount of hydrogen production as time increases. Knowing this is possibly not the case, an alternative assumption that is more likely to be valid is that it takes longer for the sample to reach a plateau with TEOA as the sacrificial reductant.

Table 6. A time profile for the photocatalytic production of hydrogen using [k³-Co(II)-SeNSeBr₂] in dimethylformamide (DMF) with $[Ru(bpy)_3]^{2+}$ as the photosensitizer. Distilled water (H_2O) was used as the proton source. The electron donor used was 1 mL of triethanolamine (TEOA). Irradiation with 450 nm lights was conducted on solution under a nitrogen atmosphere. The lights were positioned at each of the four corners coming from the sides to the vials.

[1] (μmol)	$Ru(bpy)_3^{2+}$ (μmol)	Solvent	Electron Donor	Additive	Irradiation Time	H_2 (μmol)
1	1	DMF	TEOA	H_2O (0.2 mL)	2 hr	5.545
1	1	DMF	TEOA	H_2O (0.2 mL)	4 hr	4.780
1	1	DMF	TEOA	H_2O (0.2 mL)	6 hr	18.188
1	1	DMF	TEOA	H_2O (0.2 mL)	24 hr	93.222
1	1	DMF	TEOA	H_2O (0.2 mL)	48 hr	160.350

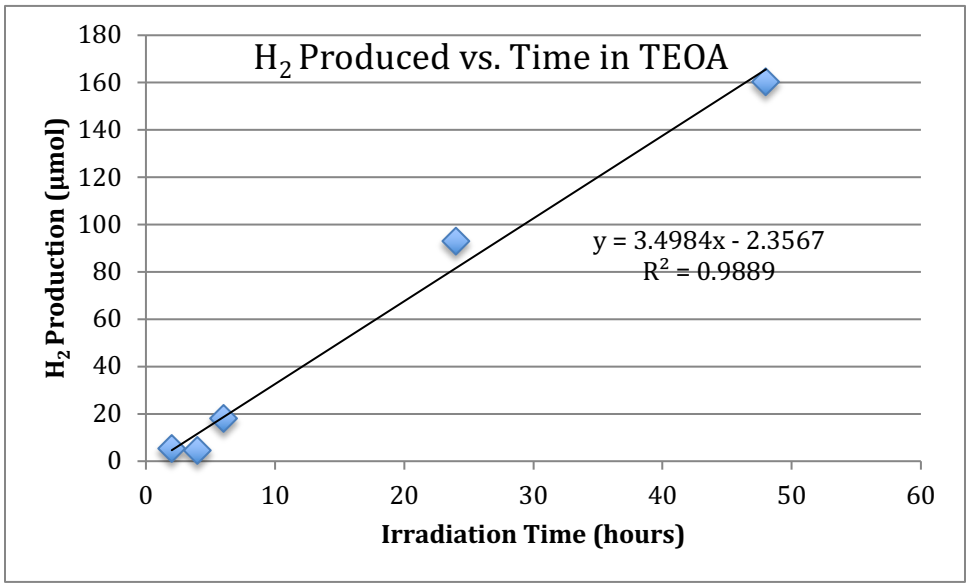

Scheme 9. A time profile for the photocatalytic production of hydrogen using [k³-Co(II)-SeNSeBr₂] in dimethylformamide (DMF) with $[Ru(bpy)_3]^{2+}$ as the photosensitizer. Distilled water (H_2O) was used as the proton source. The electron donor used was 1 mL of triethanolamine (TEOA). Irradiation with 450 nm lights was conducted on solution under a nitrogen atmosphere. The lights were positioned at each of the four corners coming from the sides to the vials.

A smaller time profile was done with the catalyst nanoparticle **2** with BNAH as the sacrificial reductant, which can be seen in Table 7. Comparing the hydrogen production from 24 hours to 48 hours shows about a 21% increase, which falls in

previous remarks made that there is a positive relationship between time and hydrogen generation, as irradiation time increases, hydrogen production also increases.

Table 7. Summary of the results for the photocatalytic production of hydrogen using Cobalt Oxide (CoO_x) Nanoparticles in dimethylformamide (DMF) with $[Ru(bpy)_3]^{2+}$ as the photosensitizer. Distilled water (H_2O) was used as the proton source. The electron donor used was 1 mmol of 1-benzyl-1,4-dihydronicotinamide (BNAH). Irradiation with 450 nm lights was conducted on solution under a nitrogen atmosphere. The lights were positioned at each of the four corners coming from the sides to the vials.

[2] (mg)	$Ru(bpy)_3^{2+}$ (μmol)	Solvent	Electron Donor	Additive	Irradiation Time	H_2 (μmol)
100	1	DMF	BNAH	H_2O (0.2 mL)	24 hr	51.388
100	1	DMF	BNAH	H_2O (0.2 mL)	48 hr	65.422

Comparing the irradiation time of 48 hours for catalyst **1** and **2** in similar conditions seen in Table 5 and 7 respectively shows that the values are very similar. The homogeneous catalyst **1** generated 62.801 μmol of hydrogen in 48 hours, while the nanoparticle catalyst **2** produced 65.422 μmol of hydrogen in 48 hours. This is further evidence that the precipitate formed from the homogeneous catalyst after irradiation is likely to be the key source of catalysis.

3.3.3. *Effect of Proton Source*

The proton source is a vital component in causing the production of hydrogen gas in a photocatalytic reaction. In the present investigation, the proton source is water since it is both environmentally friendly and relatively abundant. Water is photocatalytically reduced into hydrogen gas, which is analyzed by gas

chromatography. The effect of water was explored on photocatalytic activity with both BNAH and TEOA as the sacrificial donor.

With BNAH, a series of samples were tested with varying amounts of water as seen in Table 8. There is a positive relationship between the amount of water being used as the proton source and the production of hydrogen. When graphed, the relationship is shown to be quadratic as seen in Scheme 10. This correlation is coherent since water being the hydrogen source, it is a reasonable assumption and an affirmation that as the original source of hydrogen is increased, which in this case is water, there would also be an increase in the amount of hydrogen gas generated.

Table 8. Summary of the results for the photocatalytic production of hydrogen using [k^3-Co(II)-$SeNSeBr_2$] in dimethylformamide (DMF) with $[Ru(bpy)_3]^{2+}$ as the photosensitizer. Distilled water (H_2O) was used as the proton source. The electron donor used was 1 mmol of 1-benzyl-1,4-dihydronicotinamide (BNAH) or 1 mL of triethanolamine (TEOA). Irradiation with 450 nm lights was conducted on solution under a nitrogen atmosphere for 24 hours. The lights were positioned at each of the four corners coming from the sides to the vials.

[1] (μmol)	$Ru(bpy)_3^{2+}$ (μmol)	Solvent	Electron Donor	Additive	Irradiation Time	H_2 (μmol)
1	1	DMF	BNAH	-	24 hr	26.270
1	1	DMF	BNAH	H_2O (0.2 mL)	24 hr	29.765
1	1	DMF	BNAH	H_2O (0.5 mL)	24 hr	43.513
1	1	DMF	BNAH	H_2O (1 mL)	24 hr	76.088
1	1	DMF	TEOA	-	24 hr	177.805
1	1	DMF	TEOA	H_2O (0.2 mL)	24 hr	93.222

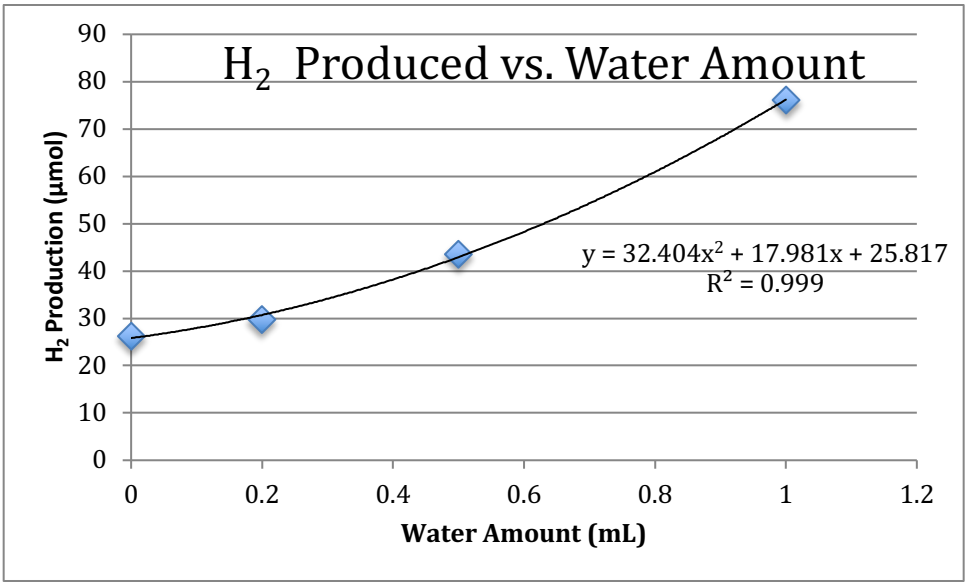

Scheme 10. The relationship between the photocatalytic production of hydrogen and amount of water used with [k³-Co(II)-SeNSeBr₂] in dimethylformamide (DMF) and $[Ru(bpy)_3]^{2+}$ as the photosensitizer. Distilled water (H_2O) was used as the proton source. The electron donor used was 1 mmol of 1-benzyl-1,4-dihydronicotinamide (BNAH). Irradiation with 450 nm lights was conducted on solution under a nitrogen atmosphere for 24 hours. The lights were positioned at each of the four corners coming from the sides to the vials.

The samples that contain TEOA raise a huge concern as seen in Table 8. With no water, which is presumptuously the hydrogen source, generates almost 50% more hydrogen than with water. This unusual result is likely caused by the effect of TEOA. TEOA has three ionisable hydrogens from its hydroxyl groups, which is possibly acting as an additional hydrogen source in conjunction with water. Another possibility is that the TEOA used had some water remnants, meaning the TEOA was not completely anhydrous, which can explain the higher hydrogen production with TEOA. Added water with TEOA gave a smaller hydrogen production, which can be explained by a possible competition between the two reactants when combined. This competition leads to less hydrogen being reduced and thus lowers the amount of hydrogen generation. This elevated more of a concern with the variability of TEOA, which led to look at the conditions of the sample more closely. This held as an

initiation period to take on the avenue of using the heterogeneous cobalt oxide nanoparticles as a catalyst. It also led to the cautious use of TEOA as a sacrificial donor, which in turn subjected subsequent samples to lean toward using BNAH as the primary electron donor.

3.3.4. *Effect of Sacrificial Donor*

The sacrificial donor is the source of the electrons that enhance the rate of photocatalytic reactions by reducing the recombination of photogenerated electrons and holes[4]. Sacrificial donors are a crucial requirement for photocatalysis; however, different donors will behave differently and have different reducing powers. The effect of the sacrificial donor was studied using BNAH, TEA and TEOA. Out of the three electron donors, the strongest donor is BNAH with the lowest oxidation potential of 0.57V vs SCE. After BNAH is TEA with an oxidation potential of 0.69V vs SCE. Only slightly weaker than TEA is TEOA with an oxidation potential of 0.8V vs SCE. However, the experiments using TEOA resulted in skewed results relative to the other sacrificial donors used because of the fact that TEOA was not completely anhydrous as mentioned previously.

In the absence of electron donor with **1** as the catalyst shows that there was no hydrogen produced, as seen in Table 9. However, when either BNAH or TEOA was used, there revealed to be hydrogen gas generated.

Table 9. Summary of the results for the photocatalytic production of hydrogen using [k^3-Co(II)-$SeNSeBr_2$] in dimethylformamide (DMF) with $[Ru(bpy)_3]^{2+}$ as the photosensitizer. Distilled water (H_2O) was used as the proton source. The electron donor used was 1 mmol of 1-benzyl-1,4-dihydronicotinamide (BNAH) or 1 mL of triethanolamine (TEOA). Irradiation with 450 nm lights was conducted on solution under a nitrogen atmosphere for 24 hours. The lights were positioned directly under each vial.

[1] (µmol)	$Ru(bpy)_3^{2+}$ (µmol)	Solvent	Electron Donor	Additive	Irradiation Time	H_2 (µmol)
1	1	DMF	-	H_2O (0.2 mL)	24 hr	0
1	1	DMF	BNAH	H_2O (0.2 mL)	24 hr	29.765
1	1	DMF	TEOA	H_2O (0.2 mL)	24 hr	93.222

In regards to using **2** nanoparticles as the catalyst illustrates similar results when no electron donor is used, this can be seen in Table 10. Furthermore, BNAH resulted in the most amount of hydrogen produced compared to any other electron donor combinations. Interesting to note, when a combination of electron donors is used, such as TEA/BNAH and TEOA/BNAH, there seems be less hydrogen produced than with just BNAH alone. This goes against the statement that sacrificial donors are known to aid in enhancing the rate of photocatalytic reactions. This could be ascribed as that TEA and/or TEOA is/are acting as an inhibitor to the photocatalytic activity when used in conjunction with BNAH.

Table 10. Summary of the results for the photocatalytic production of hydrogen using Cobalt Oxide (CoO_x) Nanoparticles in dimethylformamide (DMF) with $[Ru(bpy)_3]^{2+}$ as the photosensitizer. Distilled water (H_2O) was used as the proton source. The electron donor used were 1 mmol of 1-benzyl-1,4-dihydronicotinamide (BNAH), 1 mL of triethanolamine (TEOA), and/or trimethylamine (TEA). Irradiation with 450 nm lights was conducted on solution under a nitrogen atmosphere for 24 hours. The lights were positioned at each of the four corners coming from the sides to the vials.

[2] (mg)	$Ru(bpy)_3^{2+}$ (μmol)	Solvent	Electron Donor	Additive	Irradiation Time	H_2 (μmol)
100	1	DMF	-	H_2O (0.2 mL)	24 hr	0
100	1	DMF	BNAH	H_2O (0.2 mL)	24 hr	51.388
100	1	DMF	TEA	H_2O (0.2 mL)	24 hr	3.824
100	1	DMF	TEA/BNAH	H_2O (0.2 mL)	24 hr	2.329
100	1	DMF	TEOA	H_2O (0.2 mL)	24 hr	8.596
100	1	DMF	TEOA/BNAH	H_2O (0.2 mL)	24 hr	14.079

The effect of sacrificial donors, as seen in both Table 9 and 10, show that an electron donor is one of the necessary components that can significantly impact the yield of hydrogen.

3.3.5. *Effect of Photosensitizer*

Photosensitizers are essential to subject the irradiated light and water through photocatalytic water splitting, converting water into hydrogen and oxygen. The effect of a photosensitizer was studied with both catalyst **1** and **2** using BNAH as the electron donor.

In Table 11, in the absence of the $Ru(bpy)_3^{2+}$ photosensitizer with **1** as the catalyst shows that there was no hydrogen produced. Conversely, the presence of the $Ru(bpy)_3^{2+}$ photosensitizer showed to produce hydrogen gas.

Table 11. Summary of the results for the photocatalytic production of hydrogen using [k^3-Co(II)-$SeNSeBr_2$] in dimethylformamide (DMF) with $[Ru(bpy)_3]^{2+}$ as the photosensitizer. Distilled water (H_2O) was used as the proton source. The electron donor used was 1 mmol of 1-benzyl-1,4-dihydronicotinamide (BNAH). Irradiation with 450 nm lights was conducted on solution under a nitrogen atmosphere for 24 hours. The lights were positioned at each of the four corners coming from the sides to the vials.

[1] (μmol)	$Ru(bpy)_3^{2+}$ (μmol)	Solvent	Electron Donor	Additive	Irradiation Time	H_2 (μmol)
1	-	DMF	BNAH	H_2O (0.2 mL)	24 hr	0
1	1	DMF	BNAH	H_2O (0.2 mL)	24 hr	29.765

Similarly, in regards to using **2** nanoparticles as the catalyst shows when no $Ru(bpy)_3^{2+}$ photosensitizer is used there is no hydrogen production, which can be seen in Table 12. In contrast, the presence of the $Ru(bpy)_3^{2+}$ photosensitizer showed to produce hydrogen gas.

Table 12. Summary of the results for the photocatalytic production of hydrogen using Cobalt Oxide (CoO_x) Nanoparticles in dimethylformamide (DMF) with $[Ru(bpy)_3]^{2+}$ as the photosensitizer. Distilled water (H_2O) was used as the proton source. The electron donor used was 1 mmol of 1-benzyl-1,4-dihydronicotinamide (BNAH). Irradiation with 450 nm lights was conducted on solution under a nitrogen atmosphere for 24 hours. The lights were positioned at each of the four corners coming from the sides to the vials.

[2] (mg)	$Ru(bpy)_3^{2+}$ (μmol)	Solvent	Electron Donor	Additive	Irradiation Time	H_2 (μmol)
100	-	DMF	BNAH	H_2O (0.2 mL)	24 hr	0
100	1	DMF	BNAH	H_2O (0.2 mL)	24 hr	51.388

3.3.6. *Effect of Solvent*

Solvent is required in allowing components of the photocatalytic sample to be soluble. More often than not, an organic sample is required since most catalysts, photosensitizers, and/or sacrificial reductants are organic. The effect of solvent was studied using either DMF or ethanol as the solvent with cobalt oxide nanoparticles

as the catalyst and BNAH as the electron donor. Ethanol is especially attractive due to its renewable nature since it can be produced in high yield by fermentation of crops and thus, has a negligible contribution into the overall carbon dioxide production[26].

Comparing the results seen in Table 13 displays that there is a 90% increase in hydrogen gas generation in the presence of DMF compared to in the absence of organic solvent. Correspondingly, there is a 33% increase in hydrogen gas production in the presence of ethanol compared to in the absence of organic solvent.

Table 13. Summary of the results for the photocatalytic production of hydrogen using Cobalt Oxide (CoO_x) Nanoparticles in no organic solvent, dimethylformamide (DMF), or ethanol (EtOH) with $[Ru(bpy)_3]^{2+}$ as the photosensitizer. Distilled water (H_2O) was used as the proton source. The electron donor used was 1 mmol of 1-benzyl-1,4-dihydronicotinamide (BNAH). Irradiation with 450 nm lights was conducted on solution under a nitrogen atmosphere for 24 hours. The lights were positioned at each of the four corners coming from the sides to the vials.

[2] (mg)	$Ru(bpy)_3^{2+}$ (μmol)	Solvent	Electron Donor	Additive	Irradiation Time	H_2 (μmol)
100	1	-	BNAH	H_2O (3 mL)	24 hr	4.917
100	1	DMF	BNAH	H_2O (0.2 mL)	24 hr	51.388
100	1	EtOH	BNAH	H_2O (2 mL)	24 hr	7.332

The effect of organic solvent, as seen in Table 13, show that organic solvents are a essential component that can significantly impact the yield of hydrogen production.

3.3.7. *Effect of Catalyst*

The catalyst is arguably the most important factor in any chemical reaction. It increases the rate of the photocatalytic reaction by substantially lowering activation energy and increasing speed at which the reactants are converted into the final

product, which in this case is hydrogen. The effect of a catalyst on photocatalytic activity was observed by using catalyst **1** and **2**.

Comparing the results seen in Table 14 shows that there is a significant increase of about 92% in hydrogen gas generation in the presence of the cobalt (II) Se-N-Se catalyst compared to in the absence of catalyst.

Table 14. Summary of the results for the photocatalytic production of hydrogen using [k^3-Co(II)-$SeNSeBr_2$] in dimethylformamide (DMF) with $[Ru(bpy)_3]^{2+}$ as the photosensitizer. Distilled water (H_2O) was used as the proton source. The electron donor used was 1 mmol of 1-benzyl-1,4-dihydronicotinamide (BNAH). Irradiation with 450 nm lights was conducted on solution under a nitrogen atmosphere for 24 hours. The lights were positioned at each of the four corners coming from the sides to the vials.

[1] (µmol)	$Ru(bpy)_3^{2+}$ (µmol)	Solvent	Electron Donor	Additive	Irradiation Time	H_2 (µmol)
-	1	DMF	BNAH	H_2O (0.2 mL)	24 hr	2.491
1	1	DMF	BNAH	H_2O (0.2 mL)	24 hr	29.765

Similarly, the results seen in Table 15 shows that there is a substantial increase of about 95% in hydrogen gas generation in the presence of the cobalt oxide nanoparticle, catalyst **2**, when compared to the absence of catalyst.

Table 15. Summary of the results for the photocatalytic production of hydrogen using Cobalt Oxide (CoO_x) Nanoparticles in dimethylformamide (DMF) with $[Ru(bpy)_3]^{2+}$ as the photosensitizer. Distilled water (H_2O) was used as the proton source. The electron donor used was 1mmol of 1-benzyl-1,4-dihydronicotinamide (BNAH). Irradiation with 450 nm lights was conducted on solution under a nitrogen atmosphere for 24 hours. The lights were positioned at each of the four corners coming from the sides to the vials.

[2] (mg)	$Ru(bpy)_3^{2+}$ (µmol)	Solvent	Electron Donor	Additive	Irradiation Time	H_2 (µmol)
-	1	DMF	BNAH	H_2O (0.2 mL)	24 hr	2.491
100	1	DMF	BNAH	H_2O (0.2 mL)	24 hr	51.388

When the samples containing the catalysts from Table 14 and 15 are compared, the nanoparticle catalyst generated approximately 42% more hydrogen gas than when using cobalt (II) Se-N-Se catalyst. The cobalt oxide nanoparticles have a pronounced effect on the amount of hydrogen produced, more so than the homogeneous cobalt (II) catalyst. This affirms the hypothesis that the homogeneous catalyst was hindering the maximum potential of hydrogen production because of the constant formation of potential catalyst precipitate. This encouraged subsequent reactions to be done in similar conditions with using the heterogeneous catalyst instead.

4. Conclusion and Future Directions

In search for an effective alternate fuel source, cobalt (II) Se-N-Se catalyst was successfully synthesized and the crystal structure was obtained through X-ray diffraction analysis. However, under photocatalytic conditions a concerning black precipitate, which was theorized to be cobalt (II) hydroxide, was consistently being formed at the end of irradiation. This led to the avenue of exploring heterogeneous catalysts as an alternative catalyst source, predominantly nanostructured cobalt oxide. The nanoparticle, Co_3O_4, was synthesized and its size and structure was affirmed using X-ray powder diffraction analysis. Photocatalytic activity showed Co_3O_4 nanoparticles had a pronounced effect on the hydrogen yield. The hydrogen yield increased significantly by about 42% when compared to the homogeneous catalyst. Photocatalytic conditions also showed light intensity and absorption; irradiation time; amount of proton source; and presence of sacrificial reductant, photosensitizer, and organic solvent all play a key role in the success and yield of hydrogen gas generation.

Future studies with this project include ensuring reproducibility with the data obtained as well as doing additional experiments to further understand and characterize elements of the photosystem used. Supplementary data with reducing agents should be done to not only understand the roles of the ones previously used, but also experiment with different types such as 1,3-dimethyl-2-phenyl-2,3-dihydro-1H-benzo[d]imidazole (BIH), which is known be an effective and strong electron donor[27]. In addition, investigating new organic photosensitizers without a metal center can be done in order to lean towards a cleaner photosystem. Future

research will be focused on using nanoparticles because of the seen success with the Co_3O_4 nanoparticle catalyst and it remains relatively new in the field of hydrogen generation.

This study has insightful impacts of furthering the exploration cobalt nanoparticles as a means of a cost efficient and clean catalyst in hydrogen production of photocatalytic water splitting.

References

1. *BP Statistical Review of World Energy*, BP P. L. C. 2019.
2. REthinking Energy 2017: *Accelerating the Global Energy Transformation, International Renewable Energy Agency (IRENA)*, 2017.
3. Listorti, A.; Durrant, J.; Barber, J. Artificial Photosynthesis: Solar to fuel. *Nature Materials*. 2009, 8 (12), 929-930.
4. Reginato, G.; Zani, L.; Calamante, M.; Mordini, A.; Dessí, A. Dye-Sensitized Heterogeneous Photocatalysts for Green Redox Reactions. *European Journal of Inorganic Chemistry*. 2019, 2020 (11-12), 899-917.
5. Miseki, A.; Kudo, Y. Heterogeneous photocatalyst materials for water splitting. *Chemical Society Review*. 2009, 38 (1), 253–278.
6. Osterloh, F. E. Photocatalysis versus Photosynthesis: A Sensitivity Analysis of Devices for Solar Energy Conversion and Chemical Transformations. *ACS Energy Letters*. 2017, 2 (2), 445–453.
7. Ager, J. W.; Shaner, M. R.; Walczak, K. A.; Sharp, I. D.; Ardo S. Experimental Demonstrations of Spontaneous, Solar Driven Photoelectrochemical Water Splitting. *Energy Environment Science*. 2015, 8 (10), 2811–2824.
8. Idriss, H. The elusive photocatalytic water splitting reaction using sunlight on suspended nanoparticles: is there a way forward?. *Catalysis Science & Technology*. 2020, 10 (2), 304-310.
9. Rao, G. K.; Pell, W.; Gabidullin, B.; Korobkov, I.; Richeson, D. Electro- and Photocatalytic Generation of H_2 Using a Distinctive CoII "PN_3P" Pincer Supported Complex with Water or Saturated Saline as a Hydrogen Source. *Chemistry - A European Journal.* 2017, *23* (66), 16763–16767.
10. Rutherford, A. W.; Boussac, A. Water Photolysis in Biology. *Science*. 2004, 303 (5665), 1782-1784.
11. Barber, J. Photosystem II: Its function, structure, and implications for artificial photosynthesis. *Biochemistry (Moscow)*. 2014, 79 (3), 185-196.
12. Mangrulkar, P. A.; Joshi, M. M.; Tijare, S. N.; Polshettiwar, V.; Labhsetwar, N. K.; Rayalu, S. S. Nano cobalt oxides for photocatalytic hydrogen production. *Journal of Hydrogen Energy*. 2012, 37 (13), 10462-10466.
13. Fujishima, A.; Honda, K.; Electrochemical photolysis of water at a semiconductor electrode. *Nature*. 1972, 238 (5358), 37-38.
14. Yao Y. Y. The oxidation of hydrocarbons and CO over metal oxides: III. Co_3O_4. *Journal of Catalyst*. 1974, 33 (1), 108-122.
15. Dekker, N. J.; Hoorn, J. A.; Stegenga, S.; Kapteijn, F.; Moulijn, J. A. Kinetics of CO oxidation over Co_3O_4/Al_2O_3. *AIChE Journal*. 1992, 38 (3), 420-440.
16. Zhu, J.; Gui, Z. From layered hydroxide compounds to labyrinth-like NiO and Co_3O_4 porous nanosheets. *Materials Chemistry and Physics*. 2009, 118 (1), 243-248.
17. Watanabe, M.; Yamashita, H.; Chen, X.; Yamanaka. J.; Kotobuki, M.; Suzuki, H.; Uchida, H. Nano-sized Ni particles on hollow alumina ball: Catalysts for hydrogen production. *Applied Catalysis B: Environmental*. 2007, 71 (3-4), 237-245.
18. Losse, S.; Vos, J. G.; Rau, S. Catalytic hydrogen production at cobalt centres. *Coordination Chemistry Reviews*. 2010, 254 (21-22), 2492-2504.

19. Charvin, P.; Abanades, S.; Flamant, G.; Neveu, P.; Lemort, F. Screening and testing of promising solar thermochemical water splitting cycles for hydrogen production. WHEC 16/ 13-16 June 2006 – Lyon France.
20. Kodama, T.; Gokon, N. Thermochemical cycles for high temperature solar hydrogen production. *Chemical Reviews*. 2007, 107 (10), 4048-4077.
21. Artero, V.; Chavarot-Kerlidou, M.; Fontecave, M. Splitting water with cobalt. *Angewandte Chemie International Edition in English*. 2011, 50 (32), 7238-7266.
22. Das, D.; Rao. G. K.; Singh, A. K. Palladium(II) Complexes of the First Pincer (Se,N,Se) Ligand, 2,6-Bis((phenylseleno)methyl)pyridine (L): Solvent-Dependent Formation of [PdCl(L)]Cl and Na[PdCl(L)][PdCl4] and High Catalytic Activity for the Heck Reaction. *Organometallics*. 2009, 28 (20), 6054-6058.
23. Yang, H.; Hu, Y.; Zhang, X.; Qiu, G. Mechanochemical Synthesis of Cobalt Oxide Nanoparticles. *Materials Letters*. 2003, 58 (004), 387-389.
24. Speakman, S. A. Estimating Crystallite Size Using XRD. Presentation presented at the: MIT Center for Materials Science and Engineering. 2008.
25. Rafferty J. Beer's Law. Britannica. https://www.britannica.com/science/wave-physics. Published 2009. Accessed April 17, 2020.
26. Sheng, P.Y.; Chiu, W.W.; Yee, A.; Morrison, S.J.; Idriss, H. Hydrogen production from ethanol over bimetallic Rh-M/CeO_2 (M = Pd or Pt). *Catalysis Today*. 2007, 129 (3-4), 313-321.
27. Tamaki, Y.; Koike, K.; Ishitani, O. Highly efficient, selective, and durable photocatalytic system for CO2 reduction to formic acid. Chemical Science. 2015, 6 (12), 7213-7221.